INTERNATIONAL JOURNAL FOR NUMERICAL METHODS IN FLUIDS, VOL. 4, 685–699 (1984)

# ON A FAMILY OF STOKES FLOWS

M. B. ZATURSKA AND W. H. H. BANKS

*School of Mathematics, University of Bristol, Bristol, U.K.*

## SUMMARY

A family of simple Stokes flows involving sliding surfaces adjacent to surfaces at rest is considered. Principally, two specific flow configurations are investigated: (i) that arising when parts of the boundary of an infinitely long circular cylinder are rotating about the axis while other parts of the boundary are at rest, and (ii) the flow produced when a cap of a sphere is held at rest while the remainder of the sphere rotates about the symmetry axis. In each case computer plots of streamlines or constant velocity lines are presented to give a general impression of the resulting flow pattern.

KEY WORDS Stokes Flows

## 1. INTRODUCTION

Fluid motions in which inertia effects are small are described as Stokes flows; the equations governing these are the Navier–Stokes equations with the inertia terms omitted, a necessary condition for their validity as approximations of the full equations being that the Reynolds number, $R$, is small ($R = lU/\nu$, where $l$, $U$ are appropriate length and velocity scales and $\nu$ is kinematic viscosity). Such approximate solutions may not be uniformly valid, in which case another solution, valid in the appropriate region and matching onto the Stokes solution, is required. The archetypal problem in this context concerns uniform flow past a sphere.[1] Since the viscous shear terms are assumed large in the Stokes approximation, the theory is applicable to the subject of lubrication and hence is of practical importance.

The governing Stokes flow equations are thus

$$\nabla^2\boldsymbol{\omega} = 0, \qquad \nabla \cdot \mathbf{u} = 0 \tag{1}$$

where $\boldsymbol{\omega} = \nabla \wedge \mathbf{u}$ is the vorticity. For two-dimensional motions these become, in terms of a stream function $\psi$,

$$\nabla^2(\nabla^2\psi) = 0 \tag{2}$$

where $\nabla^2$ represents the two-dimensional Laplacian.

We present the Stokes solutions for a number of problems: in Section 2 superposition is used to generalize a well-known solution involving a moving plane. Section 3 is concerned with fluid motion generated by a rotating circular cylinder with fixed shields, and in Section 4 we consider flows generated by a sphere, part of which is rotating and the remainder at rest. Computer plots of either streamlines or constant velocity lines supplement the analytical solutions. The software permitted variation in grid size thereby allowing accuracy checks; however the results should be viewed as providing an overall picture of the flow.

0271–2091/84/070685–15$01.50

*Received November 1982*
*Revised 29 June 1983*

The stimulus for this work arose in preparation of supplementary work for lecture courses, but it was later felt that it was also of interest to fluid dynamicists generally, and hence merited a wider circulation.

## 2. PLANE GEOMETRY

Consider the two-dimensional Stokes flow generated by a plane at $y=0$, $x>0$, moving uniformly in the $x$-direction with speed $U$, and a stationary plane occupying $y=0$, $x<0$. The problem is a special case of a family of flows[2] and the solution of equation (2) is

$$\psi = Ur(1-\theta/\pi)\sin\theta \tag{3}$$

where $r$, $\theta$ are plane polar co-ordinates, $u_r = r^{-1}\,\partial\psi/\partial\theta$ and $u_\theta = -\partial\psi/\partial r$. The region of validity of this approximate solution is $rU/\nu \ll 1$. Hancock[3] has obtained higher order terms by perturbing about the term in (3) but our concern is solely with Stokes solutions.

The linearity of the Stokes problem and the simple geometry allow superposition of solutions where regions of validity overlap. For example, when a section, $|x|<a$, of the plane moves in the $x$-direction with speed $U$, and $Ua/\nu \ll 1$, with the remainder at rest, we obtain

$$\psi = (Uy/\pi)\{\tan^{-1}[y/(x-a)] - \tan^{-1}[y/(x+a)]\}. \tag{4}$$

Figure 1 shows the contours of $\psi\pi/(Ua)$ as a function of the dimensionless variables $x/a$, $y/a$, the fixed part of the boundary $y=0$ being indicated by a parallel line displaced slightly from its true position. The restriction on $a$ ($\ll \nu/U$) implies that (4) is a valid approximation near the slit. For $Ua/\nu = O(1)$ it is to be expected that the solution near $x=a$ is given by (3) and is of similar simple form near $x=-a$.

The solution (4) was given by Dean[4] who then considered the limiting case $a \to 0$, $U \to \infty$ where $aU$ remains finite. Then

$$\psi = 2\pi^{-1}aU\sin^2\theta \tag{5}$$

which, owing to the failure of (3) for $rU/\nu = O(1)$ cannot be regarded as giving the approximate behaviour of the Navier–Stokes solution at sufficiently large distance from the moving surface. Contours of $\pi\psi/(aU)$ are straight lines radiating from the origin and give the approximate behaviour of (4) beyond a couple of gap widths from the origin. The solution

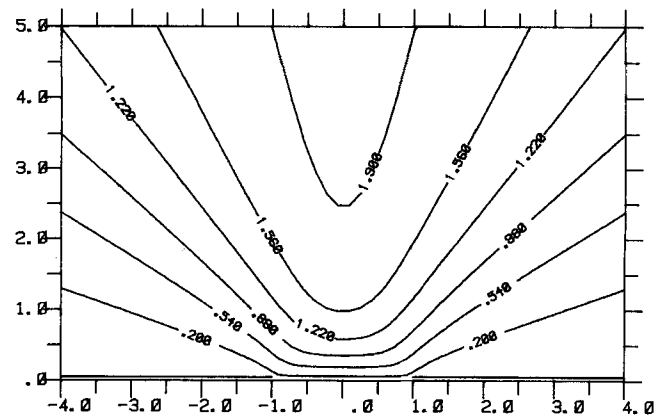


Figure 1. Contours of $\psi\pi/(Ua)$ from (4). The flow is generated by a section of the wall moving in its own plane

$\psi = A \sin^2 \theta$ is a uniformly valid Stokes solution, although Dean shows that there is no solution $\psi(\theta)$ of the Navier–Stokes equations satisfying appropriate conditions on $y = 0$.

## 3. CYLINDRICAL GEOMETRY

The flows investigated here are generated by the uniform rotation, about its axis, of an infinitely long circular cylinder with a fixed infinitely long shield, or shields, over part(s) of it; the problem is thus assumed to be two-dimensional. The flow may be interior or exterior to the cylinder: the former, with one shield was first studied by Mabey[5] and later by Dean.[4]

### (a) *Single shield*

Referred to cylindrical polar co-ordinates $(r, \theta, z)$ the cylinder $r = a$ rotates about the $z$-axis with constant angular velocity $\omega$. Consider a fixed shield at $r = a$, $\alpha < \theta < 2\pi - \alpha$, so that in terms of a stream function $\psi(r, \theta)$ we seek to solve (2) subject to

$$\begin{aligned} \psi &= \text{constant} = 0, \quad \text{say} \\ \partial\psi/\partial r &= -a\omega, \qquad -\alpha < \theta < \alpha \\ &= 0, \qquad \alpha < \theta < 2\pi - \alpha \end{aligned} \tag{6}$$

on $r = a$.*

For the interior flow we find

$$\psi = (a^2\omega/2\pi)(1-\rho^2)\left(\alpha + 2\sum_1^\infty \rho^n n^{-1} \sin n\alpha \cos n\theta\right)$$

where $\rho = r/a$, or equivalently,

$$\psi = (a^2\omega/2\pi)(1-\rho^2)\left[\alpha - \tan^{-1}\left(\frac{\rho^2 \sin 2\alpha - 2\rho \sin\alpha \cos\theta}{1 - 2\rho \cos\alpha \cos\theta + \rho^2 \cos 2\alpha}\right)\right] \tag{7}$$

a form uniformly valid over the whole field. Mabey gave a geometrical construction, based on (7), for drawing the streamlines and so presented a diagram for $\alpha = \pi/2$. We have used computer graphics facilities to show streamline patterns for $\alpha = \pi/10$, $\pi/2$, $9\pi/10$: see Figures 2(a), (b), (c). The fixed part of the boundary is again indicated by a slightly displaced line. Care is needed in interpreting the arc-tangent term to ensure continuity of $\psi$. For small values of $\alpha$ (large shield) an eddy forms near the small moving portion of the boundary, its centre moving towards $r = 0$ as $\alpha$ increases, so that as $\alpha$ approaches $\pi$, the motion approaches rigid body rotation.

For $\alpha \ll 1$, equation (7) is approximated by

$$\psi \simeq a^2\omega\alpha(1-\rho^2)^2/[2\pi(1 - 2\rho\cos\theta + \rho^2)] \tag{8}$$

except for $1 - \rho = O(\alpha)$ and $\theta = O(\alpha)$. Figure 2(d) shows contours for $\alpha = \pi/10$ and we note the satisfactory agreement with Figure 2(a) away from the vicinity of the moving cylinder. The result (8) is equivalent to an expression derived by Dean who invoked the double limit $\alpha \to 0$, $V \to \infty$ with $\alpha V$ finite, where $V = a\omega$. Finally, note that the superposition of an angular velocity $-\omega$ interchanges the roles of shield and moving cylinder.

The behaviour of (8) in the neighbourhood of the moving part of the cylinder is of the form (5) corresponding to straight streamlines. The contours in Figure 2(d) are not of this form near $\rho = 1$, $\theta = 0$, due presumably to the coarseness of the grid used.

* Smith[6] has considered in detail the boundary-layer problem when the Reynolds number is large.

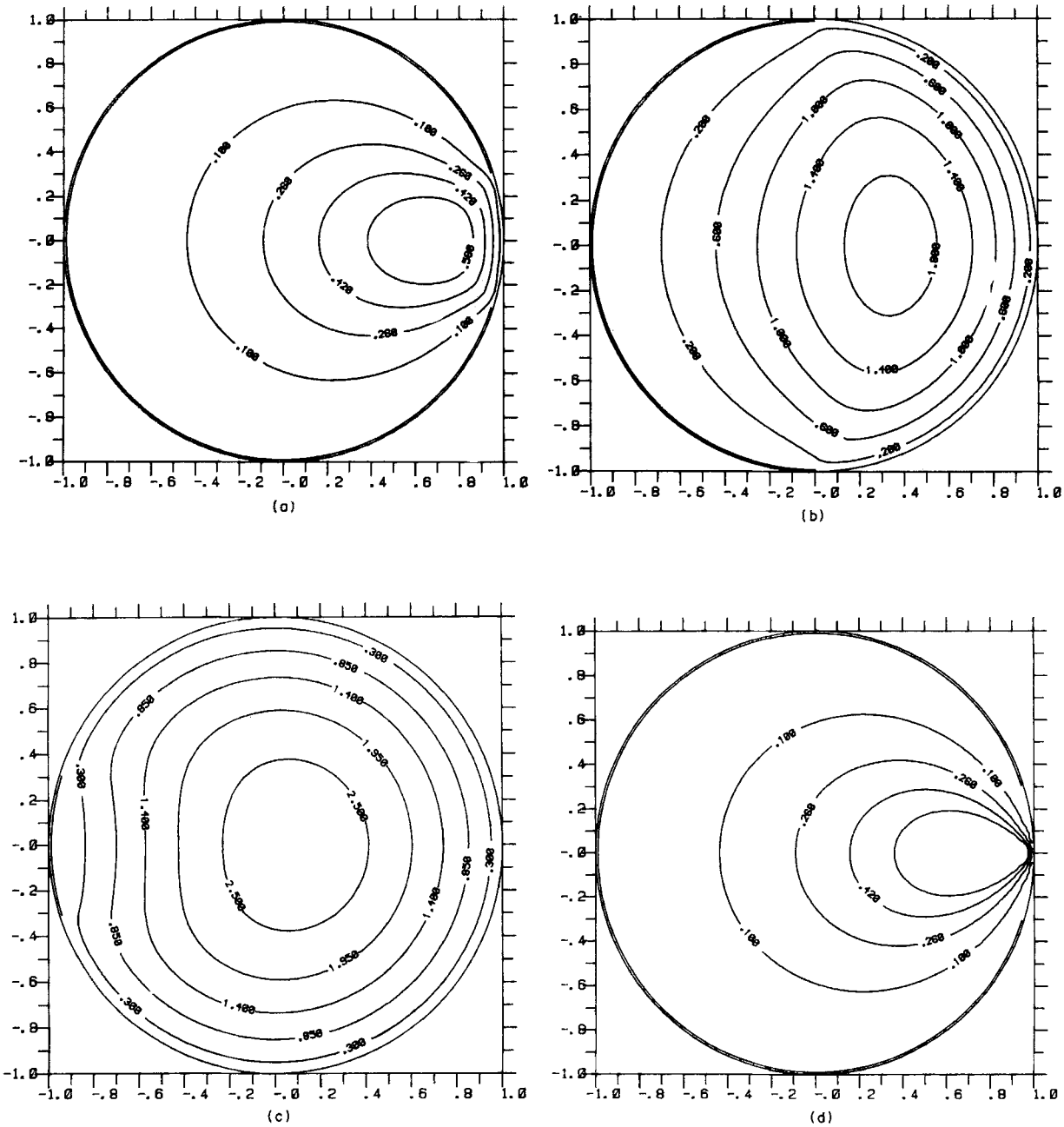


Figure 2. Single shield. Contours of $2\psi\pi/(a^2\omega)$ from (7) with (a) $\alpha = \pi/10$, (b) $\alpha = \pi/2$ and (c) $\alpha = 9\pi/10$. (d) Approximate contours from (8) for $\alpha \ll 1$ (compare with (a))

When the flow is in $r>a$ the solution of (2) subject to (6) is

$$\psi = -(a^2\omega/\pi)\left[\alpha \log \rho + \tfrac{1}{2}(1-\rho^2)\tan^{-1}\left(\frac{\sin 2\alpha - 2\rho \sin\alpha \cos\theta}{\rho^2 - 2\rho\cos\theta\cos\alpha + \cos 2\alpha}\right)\right] \tag{9}$$

which, by analogy with Section 2 is non-uniformly valid at $\infty$. Figures 3(a), (b), (c) show streamlines for typical cases of $\alpha$ small, $\alpha = \pi/2$ and $\alpha$ close to $\pi$. For $\alpha$ close to $\pi$ (small shield) the flow on the side of the cylinder opposite the shield is very similar to that when no shield is present: the streamlines are closed. For smaller values of $\alpha$ (Figures 3(a), (b)), the streamlines go off to infinity. The critical value of $\alpha$ separating the two distinct forms is given by the root of $\tan(\alpha/2) = \alpha$, i.e. $\alpha = 2{\cdot}33112$.

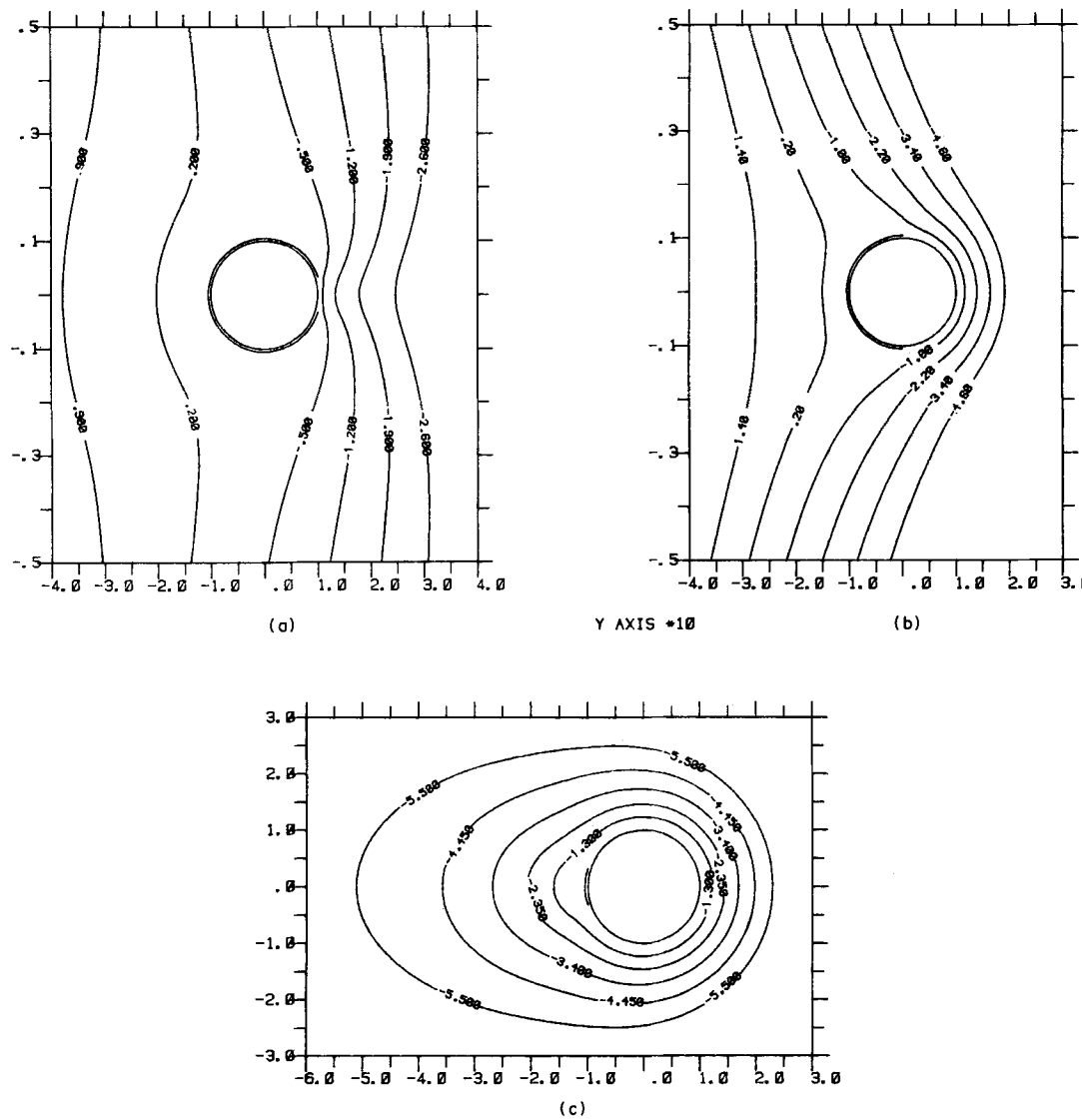


Figure 3. Single shield. Contours of $2\psi\pi/(a^2\omega)$ from (9) with (a) $\alpha = \pi/10$, (b) $\alpha = \pi/2$ and (c) $\alpha = 9\pi/10$

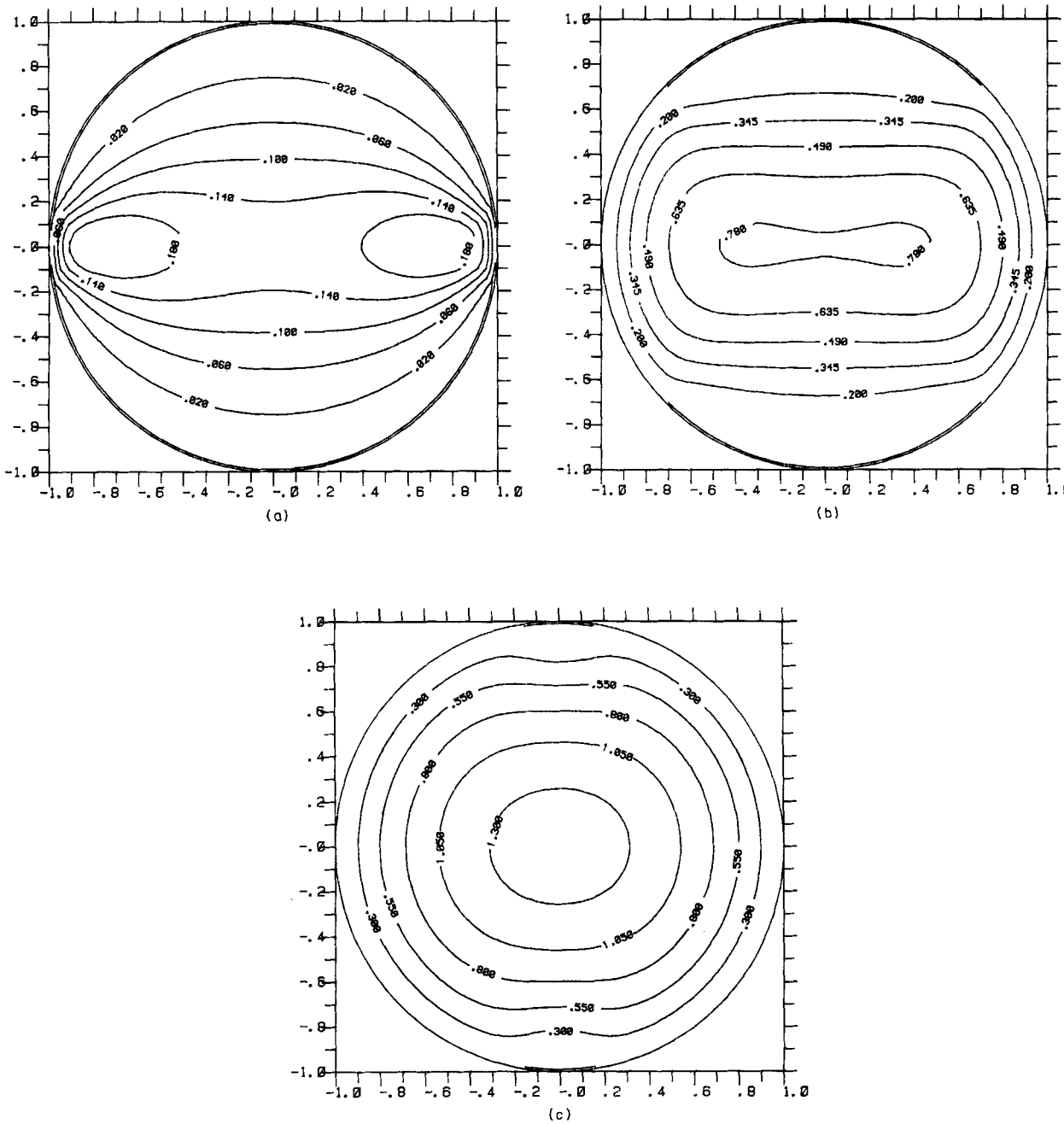


Figure 4. Two shields. Contours of $\psi\pi/(a^2\omega)$ from (11) with (a) $\alpha = \pi/20$, (b) $\alpha = \pi/4$ and (c) $\alpha = 9\pi/20$

For small values of $\alpha$, (9) is approximated by

$$\psi = -(a^2\omega\alpha/\pi)[\log\rho + (1-\rho^2)(1-\rho\cos\theta)/(\rho^2 - 2\rho\cos\theta + 1)] \tag{10}$$

except near $\rho = 1$, $\theta = 0$. Again agreement between approximate (10) and exact (9) results is good for $\alpha = \pi/10$ except in the region of $\rho = 1$, $\theta = 0$.

(b) *Two, and more, shields*

The two forms of single shield solution discussed in (a) can be used to construct slow flows caused by a rotating cylinder with any number of fixed shields, using superposition as in Section 2. In order to restrict the number of parameters we examine only symmetrically placed shields here, and no more than four shields.

First, consider the flow in $\rho \leqslant 1$ with fixed shields at $\rho = 1$, $\alpha < \theta < \pi - \alpha$ and $\pi + \alpha < \theta < 2\pi - \alpha$ where $0 < \alpha < \pi/2$. Simple superposition of solutions of the form (7) gives

$$\psi = (a^2\omega/\pi)(1-\rho^2)\left[\alpha - \tfrac{1}{2}\tan^{-1}\left(\frac{\rho^4\sin 4\alpha - 2\rho^2\sin 2\alpha\cos 2\theta}{1 - 2\rho^2\cos 2\alpha\cos 2\theta + \rho^4\cos 4\alpha}\right)\right] \tag{11}$$

which, since each of its constituents is uniformly valid, is itself so also. Figures 4(a), (b), (c) show streamlines for $\alpha = \pi/20$, $\pi/4$, $9\pi/20$. For small values of $\alpha$ two eddies form near the two small moving parts of the boundary (see Figure 4(a)): the fact that (11) is the sum of two solutions each containing an eddy is indicative of this provided that each eddy is in the relatively *weak* part of the field of the other. However, comparison of the two streamline patterns near the moving boundary when $\alpha = \pi/20$ shows reasonable agreement with either of the eddies of (11) only very close to the moving boundary (see Figure 4(a)). Batchelor's result[7] suggests that for high Reynolds number flow only one eddy would exist and hence that a critical $R$ separates the two phenomena. The Stokes flow eddies when $\alpha$ is small approach one another as $\alpha$ increases until they coalesce forming a single eddy, so that as $\alpha \to \pi/2$ the flow approaches solid body rotation (Figure 4(c)). The transition between the forms occurs when $\sin 2\alpha = \alpha$, i.e. $\alpha = 0{\cdot}94775$. For small $\alpha$

$$\psi = (a^2\omega/\pi)\alpha(1-\rho^2)^2(1+\rho^2)/(1 - 2\rho^2\cos 2\theta + \rho^4) \tag{12}$$

approximately, and again contour plots of (12) for $\alpha = \pi/20$ are very similar to the exact plot, except close to the moving cylinder where (12) fails as an approximation.

For $\rho \geqslant 1$ with the same boundary conditions

$$\psi = -(a^2\omega/\pi)\left[2\alpha\log\rho + \tfrac{1}{2}(1-\rho^2)\tan^{-1}\left(\frac{\sin 4\alpha - 2\rho^2\sin 2\alpha\cos 2\theta}{\rho^4 - 2\rho^2\cos 2\theta\cos 2\alpha + \cos 4\alpha}\right)\right] \tag{13}$$

which fails as an approximation of the Navier–Stokes quations when $\rho$ is large. Figures 5(a), (b), (c) show streamlines for $\alpha = \pi/20$, $\pi/4$, $9\pi/20$. The approximated form of (13) for small $\alpha$ gives contours almost indistinguishable from the exact form when $\alpha = \pi/20$ except near the moving cylinder where the approximation fails.

The existence of the two eddies in the interior flow with two shields led us to examine interior flows with three and four symmetrically placed shields. In the former case with shields at $\alpha < \theta < 2\pi/3 - \alpha$, $2\pi/3 + \alpha < \theta < 4\pi/3 - \alpha$ and $4\pi/3 + \alpha < \theta < 2\pi - \alpha$ the solution is

$$\psi = (a^2\omega/2\pi)(1-\rho^2)\left[3\alpha - \sum_{K=0}^{2}\tan^{-1}\left(\frac{\rho^2\sin 2\alpha - 2\rho\sin\alpha\cos\theta_K}{1 - 2\rho\cos\alpha\cos\theta_K + \rho^2\cos 2\alpha}\right)\right] \tag{14}$$

where $\theta_K = \theta + 2K\pi/3$. Streamlines for $\alpha = \pi/60$ and $\pi/6$ are shown in Figures 6(a), (b), and

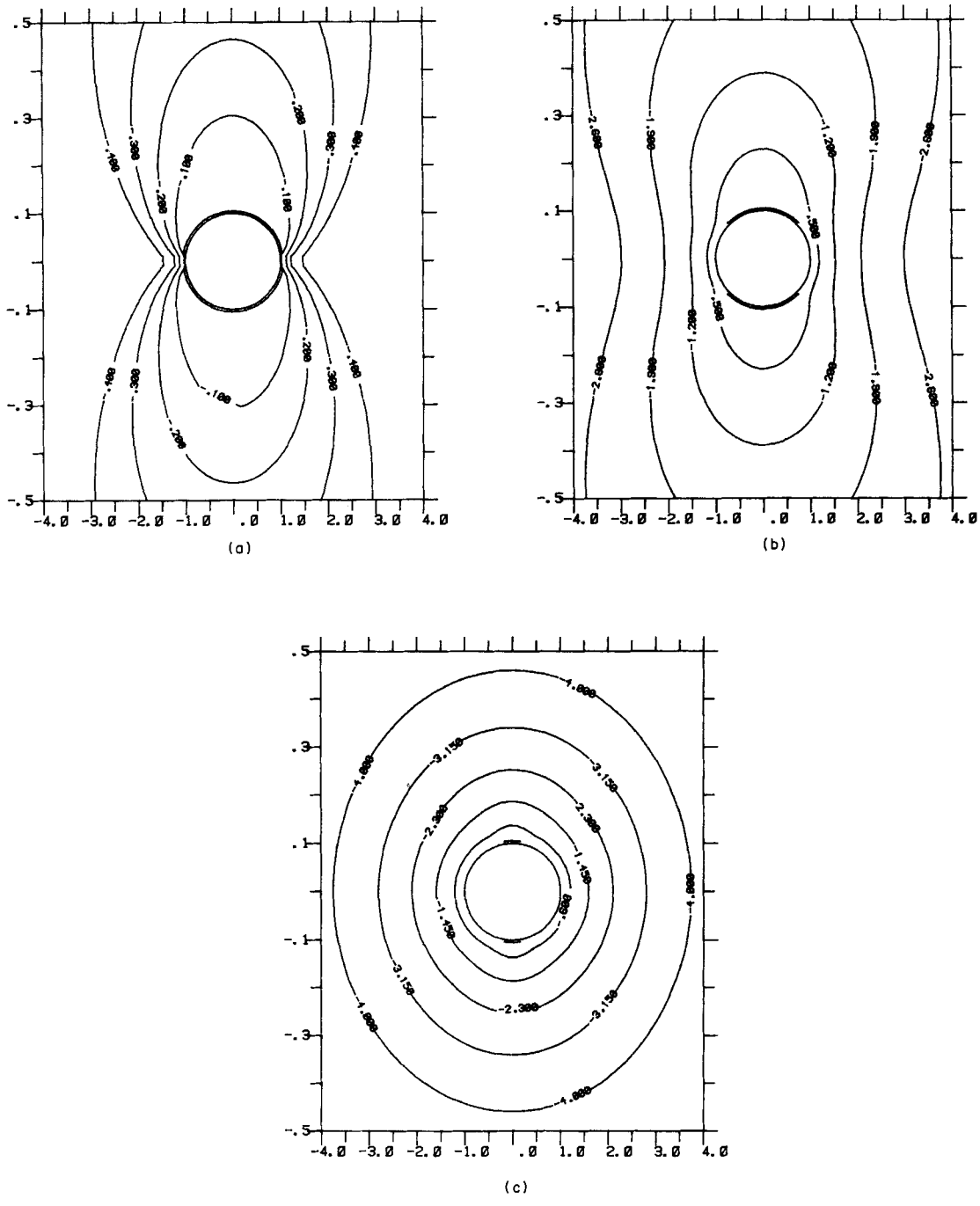


Figure 5. (a), (b), (c). Two shields. Details as for Figure 4

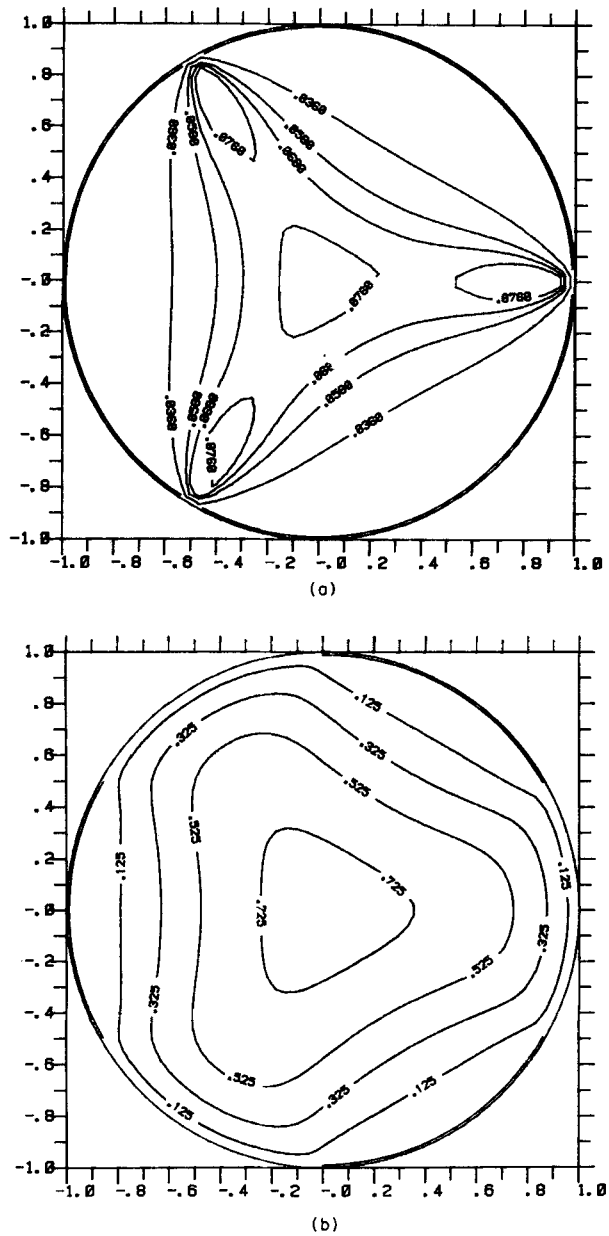


Figure 6. Three shields. Contours of $2\psi\pi/(a^2\omega)$ from (14) with (a) $\alpha = \pi/60$ and (b) $\alpha = \pi/6$

there are indeed three eddies for $\alpha = \pi/60$ but not for $\alpha = \pi/6$. The critical $\alpha$ separating the regimes has not been evaluated. The rectangular nature of the grid used by the graphics procedure explains the lack of symmetry of the streamlines in Figure 6(a) about $\theta = 0$, $2\pi/3$ and $-2\pi/3$. Figures 7(a), (b) illustrate streamlines when there are four symmetrically placed shields at $\alpha < \theta < \pi/2 - \alpha$, $\pi/2 + \alpha < \theta < \pi - \alpha$, $\pi + \alpha < \theta < 3\pi/2 - \alpha$, and $3\pi/2 + \alpha < \theta < 2\pi - \alpha$ with $\alpha = \pi/80$ and $\pi/8$: note the four eddies for small $\alpha$. For both the three and four

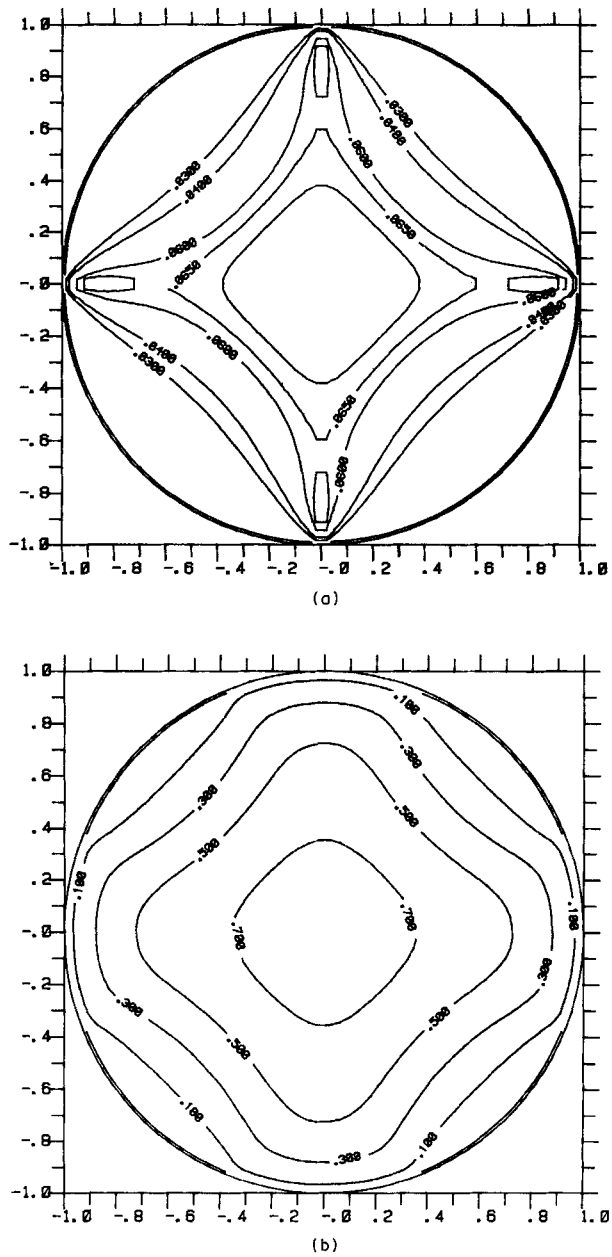


Figure 7. Four shields. Contours of $\psi\pi/(a^2\omega)$ with (a) $\alpha = \pi/80$ and (b) $\alpha = \pi/8$

shield examples agreement between exact forms and their small $\alpha$ analogues is excellent for small $\alpha$, subject to the same limitations as in previous cases.

The above solutions are zeroth order terms in expansions of $\psi$ in powers of the Reynolds number; clearly higher order terms would be tedious to calculate from them, although the small $\alpha$ forms e.g. (8) appear more tractable. However, Dean showed that an expansion with (8) as zeroth order terms fails at a later stage.

## 4. THE SPHERICAL GEOMETRY

Referred to spherical co-ordinates $(r, \theta, \phi)$, part $(\theta < \beta)$ of a sphere of radius $a$ is held at rest while the remaining cap rotates about $\theta = 0$ with constant angular velocity $\omega$. The flow may be in $r \leq a$, or $r \geq a$. The Stokes velocity field has a single component so that $v_r = v_\theta = 0$ to this order, and we assume rotational symmetry $\partial/\partial\phi \equiv 0$. Thus the Navier–Stokes equations become

$$\nabla^2 v_\phi - v_\phi/(r^2 \sin^2\theta) = 0. \tag{15}$$

The solution of (15) having no singularities at $\theta = 0, \pi$ is

$$v_\phi = \sum_0^\infty [A_m (r/a)^m + B_m (r/a)^{-m-1}] P_m^1(\cos\theta) \tag{16}$$

where $P_m^1$ is the associated Legendre function of degree $m$ and order one; for interior flows $B_m \equiv 0$, whereas for exterior flows $A_m \equiv 0$. The boundary conditions on $r = a$ are

$$\begin{aligned} v_\phi &= 0, \qquad 0 < \theta < \beta \\ &= a\omega \sin\theta, \qquad \beta < \theta < \pi. \end{aligned} \tag{17}$$

The evaluation of the $A_m, B_m$ for general $\beta$ presents some difficulty and so we confine attention to some special cases only.

For the interior flow problem with $\beta = \pi/2$ we find

$$A_1 = -a\omega/2,\ A_{2m+1} = 0, \qquad A_{2m} = a\omega(-1)^{m-1}(2m + \tfrac{1}{2})(m - 3/2)!/4\sqrt{\pi}(m+1)!$$

for $m = 1, 2, \ldots$ so that with $\rho = r/a$

$$v_\phi = \tfrac{1}{2}\rho a\omega \sin\theta - \frac{a\omega \sin\theta}{4\sqrt{\pi}} \sum_{s=1}^{\infty} \frac{(-1)^{s-1}(2s + \frac{1}{2})(s - 3/2)!}{(s+1)!} \rho^{2s} P'_{2s}(\cos\theta). \tag{18}$$

Thus $v_\phi = \frac{1}{2} r\omega$ on $\theta = \pi/2$. Figure 8(a) shows lines of constant $v_\phi/a\omega$ using the first six terms in the summation expression. The convergence of (18) is such that a larger number of terms is required in some regions; we have consequently only given a restricted plot where the effect of the sixth term is negligible, but have indicated, by broken lines, the behaviour expected near the singular point $\rho = 1$, $\theta = \pi/2$ and also in the region of $\rho = 1$, $\pi/2 < \theta < \pi$ (more detail concerning the former is given later).

Other analytically tractable problems correspond to $\beta \ll 1$ and $0 < \pi - \beta \ll 1$: these are closely related, the superpositon of an angular velocity $-\omega$ interchanging fixed and moving parts.

With $\beta \ll 1$ the solution of the interior flow problem $\rho < 1$ is

$$v_\phi = a\omega \sin\theta [\rho P'_1(\cos\theta) - (\beta^4/8) \sum_1^\infty (m + \tfrac{1}{2}) \rho^m P'_m(\cos\theta)] \tag{19}$$

approximately. The series may be summed analytically to give

$$v_\phi = a\omega\rho \sin\theta [1 - 3\beta^4(1-\rho^2)/16(1 - 2\rho\cos\theta + \rho^2)^{5/2}] \tag{20}$$

except when $\rho = 1$ and $\theta = 0$ where there is a singularity. For $0 < \pi - \beta \ll 1$ we find similarly

$$v_\phi = 3a\omega(\pi - \beta)^4 \rho(1 - \rho^2) \sin\theta/16(1 + 2\rho\cos\theta + \rho^2)^{5/2} \tag{21}$$

except at the singularity $\rho = 1$, $\theta = \pi$ where the approximation fails. Figure 8(b) shows lines

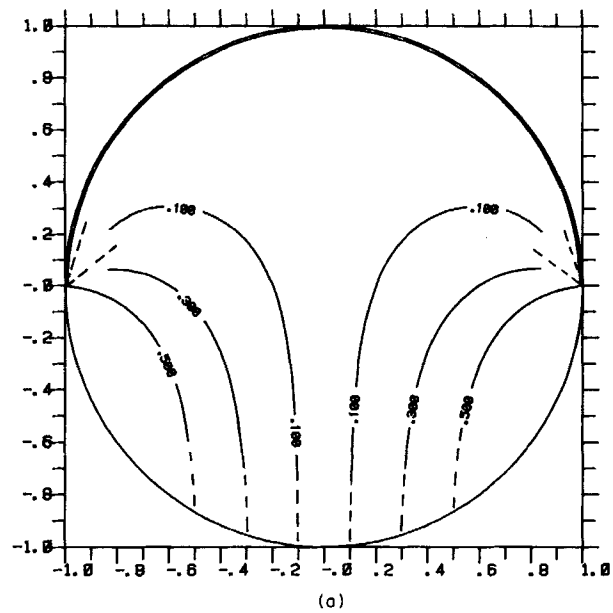


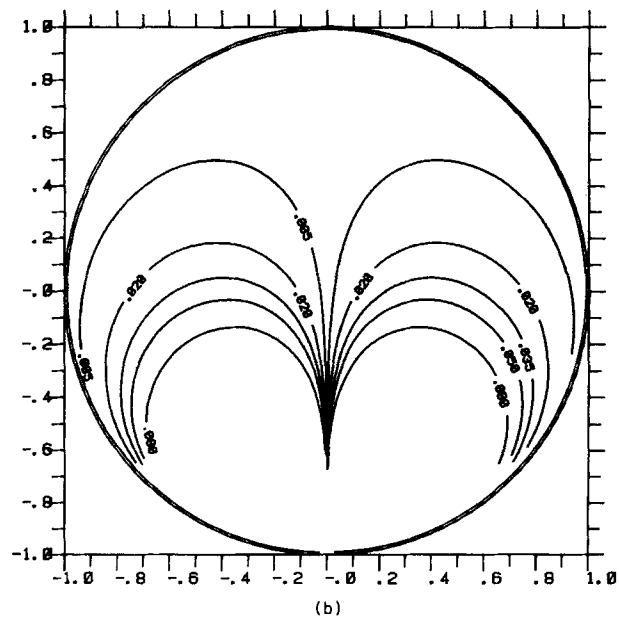


Figure 8. (a) Lines of constant $v_\phi/a\omega$, from (18), due to one hemisphere rotating and the other held fixed. See text for further information. (b) Lines of constant $10^3 v_\phi/a\omega$, from (21) due to a small cap of the sphere rotating and the remainder at rest

of constant $10^3 v_\phi/a\omega$, using (21) with $\beta = 9\pi/10$. No plot from (20) is presented as the departure from solid body rotation is extremely small for $\beta \ll 1$.

As $\beta \to \pi$ the flow pattern near $\theta = \pi$ should approach that for a small spinning disc in a fixed infinite plane. In terms of cylindrical polar co-ordinates $(r, \theta, z)$ the disc $z = 0$, $r \leq b$ spins with constant angular velocity $\Omega$; $z = 0$, $r > b$ is at rest and the fluid occupies the region $z > 0$. With $v_r = v_z = 0$ to this order, and $\partial/\partial\theta \equiv 0$, the swirl velocity satisfies $\nabla^2 v_\theta - v_\theta/r^2 = 0$ subject to boundary conditions $v_\theta = r\Omega$, $r \leq b$ and $v_\theta = 0$, $r > b$ on $z = 0$, with $v_\theta$ bounded as $z \to \infty$. This has solution

$$v_\theta = b\Omega \int_0^\infty e^{-sz/b} J_1(sr/b) J_2(s)\, ds \tag{22}$$

where $J_n$ is the Bessel function of order $n$. Hence for $r \gg b$, $z \gg b$ $v_\theta$ is given approximately by

$$v_\theta = 3\Omega b^4 rz/8(r^2 + z^2)^{5/2}. \tag{23}$$

With a suitable change of origin and interpretations of $b, \Omega$ this behaviour is equivalent to the limiting behaviour of $v_\phi$ in (21) close to $\rho = 1$, $\theta = \pi$. Figure 9 shows lines of constant $v_\theta/b\Omega$ using equation (23).

A simple uni-directional flow relevant to the first flow of this section is that generated by the semi-infinite plane $z = 0$, $y > 0$ moving parallel to the $x$-axis with speed $U$, while $z = 0$, $y < 0$ is at rest with the fluid occupying $z > 0$. The velocity, $u$, in the $x$ direction is

$$u/U = \tfrac{1}{2} + \pi^{-1} \tan^{-1}(y/z).$$

Figure 8(a) shows lines corresponding to constant $u$—these can only be applicable very close to $\rho = 1$, $\theta = \pi/2$ and although we cannot show that they represent the continuation of the constant $v_\phi$ lines there seems good evidence to suggest that they are so.

For exterior flow with boundary conditions (17) and $\beta = \pi/2$

$$v_\phi = (a\omega/2\rho^2)\sin\theta - (a\omega/4\sqrt{\pi})\sin\theta \sum_{s=1}^{\infty} (-1)^{s-1}(2s + \tfrac{1}{2})(s - 3/2)!\, \rho^{-2s-1} P'_{2s}(\cos\theta)/(s+1)! \tag{24}$$

so that $v_\phi = a\omega/2\rho^2$ on $\theta = \pi/2$. Figure 10(a) illustrates lines of constant $v_\phi/a\omega$: again we show only those parts where the effect of the last term retained in the summation is

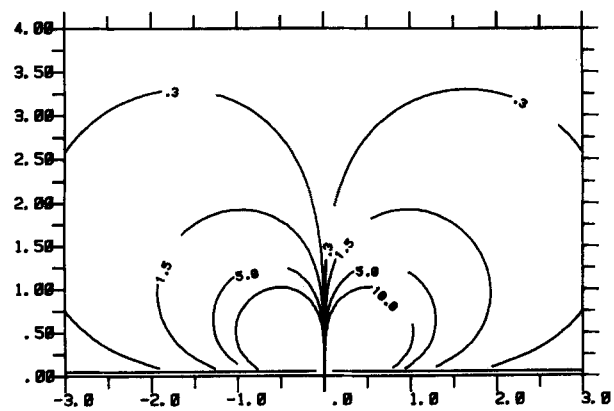


Figure 9. Lines of constant $v_\theta/b\Omega$ due to a small disc rotating in an infinite plane at rest

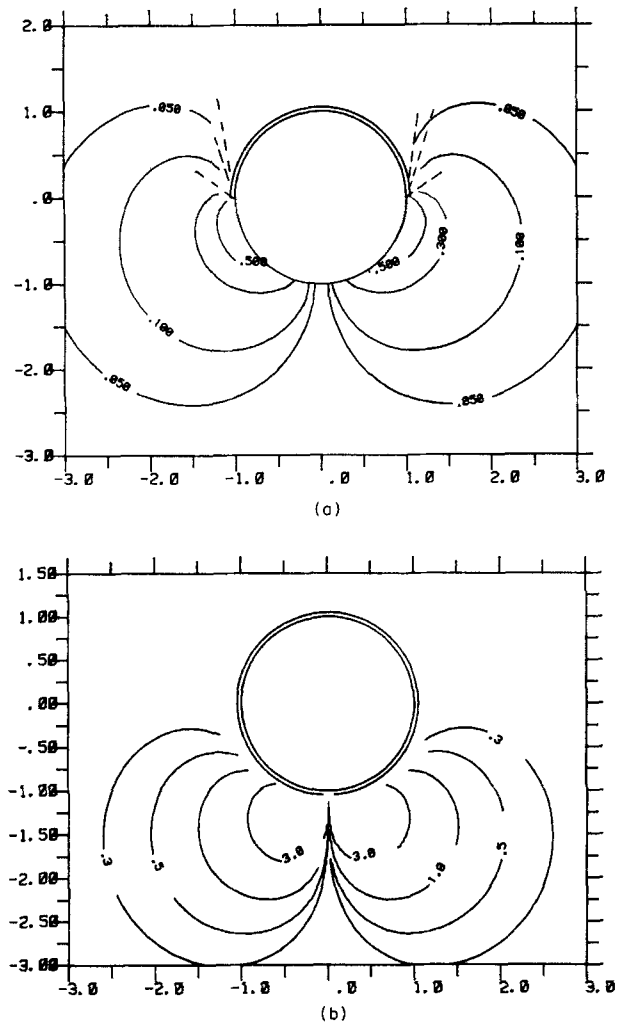


Figure 10. (a) Lines of constant $v_\phi/a\omega$, from (24), due to one hemisphere rotating and the other held fixed. See text for further information. (b) Lines of constant $10v_\phi/[a\omega(\pi-\beta)^4]$, from (26), due to a small cap of the sphere rotating and the remainder at rest

negligible. Broken lines indicate expected behaviour near $\rho = 1, \theta = \pi/2$. The poor convergence near $\rho = 1, \pi/2 < \theta < \pi$ existing in the interior problem is not noticeable on the scale of the present Figure.

For exterior flows with $\beta \ll 1$ we find

$$v_\phi = a\omega \sin\theta[\rho^{-2} - 3\beta^4\rho(\rho^2-1)/16(1-2\rho\cos\theta+\rho^2)^{5/2}] \tag{25}$$

approximately, except at $\rho = 1$, $\theta = 0$ where there is a singularity. When $0 < \pi - \beta \ll 1$, superposition gives the approximate solution

$$v_\phi = 3a\omega(\pi-\beta)^4\rho(\rho^2-1)\sin\theta/16(1+2\rho\cos\theta+\rho^2)^{5/2} \tag{26}$$

except at the singularity $\rho = 1$, $\theta = \pi$. Figure 10(b) shows lines of constant $10v_\phi/a\omega(\pi-\beta)^4$ from (26) when $\beta = 19\pi/20$; we do not plot results from (25) as the departure from the $\beta = 0$

solution is very small for $\beta \ll 1$. An appropriate shift of origin and interpretation of $b$ and $\Omega$ show that $v_\theta$ from (23) is equivalent to the limiting behaviour of $v_\phi$ in (26) when $\rho$ is close to 1 and $\theta$ to $\pi$.

## 5. DISCUSSION

The flows investigated above form part of a wider class of Stokes flows whose prototype is the Taylor solution (see e.g. Reference 2). Those of Sections 2 and 3 are analytically straightforward enough to be valuable in teaching fluid dynamics and may be approached in the sequence: (i) prediction of flow using physical intuitition, (ii) analysis and (iii) confirmation of (i). It is possible also, for example, to investigate streamlines analytically for large or small shields and in the vicinity of specific points.

Also of interest and arising from Section 3 is the possible generation of multiple eddies by boundary motions of a circular cylinder. It seems reasonable to suppose that $n$ ($>4$) sleeves of suitable size and siting would produce $n$ eddies within such a cylinder: there may be an upper bound on $n$. There is also scope for experimental verification of the predictions.

## REFERENCES

1. I. Proudman and J. R. A. Pearson, 'Expansions at small Reynolds numbers for the flow past a sphere and a circular cylinder', *J. Fluid Mech.*, **2** 236–262 (1957).
2. G. K. Batchelor, *An Introduction to Fluid Mechanics*, Cambridge University Press, 1967.
3. C. Hancock, 'Corner flows', *Ph.D. thesis*, University of Bristol, 1981.
4. W. R. Dean, 'A shearing motion of viscous liquid', *Mathematika*, **14** 125–131 (1967).
5. D. G. Mabey, 'The formation and decay of vortices', *M.Sc. thesis*, University of London, 1954.
6. E. G. Smith, 'Discontinuities in boundary conditions in laminar boundary layer flow with closed streamlines', *Ph.D. thesis*, University of Bristol 1977.
7. G. K. Batchelor, 'On steady laminar flow with closed streamlines at large Reynolds number', *J. Fluid Mech.*, **1** 177–190 (1956).